Multi-Objective Intelligent Control of Bi-Directional V2X Charging Using NSGA-II in an Integrated Energy Management System

Muhammad Aqmal Bin Abu Hassan[1], Ezmin Abdullah[2]*, Muhammad Umair[3],
Nik Hakimi Nik Ali[4], Roslina Mohamad[5], Nabil M. Hidayat[6]
Energy Solution & Computation Laboratory (ESCO), Universiti Teknologi MARA, Shah Alam, Selangor, Malaysia [1, 2, 6]
Wireless High-Speed Network Research Interest Group (RIG),
Universiti Teknologi MARA, 40000 Shah Alam, Selangor, Malaysia [2, 5]
Faculty of Electrical Engineering, Universiti Teknologi MARA, Shah Alam, Selangor, Malaysia [1, 2, 3, 4, 5, 6]

Abstract—**This study presents the development and evaluation of an intelligent control system for a real-time bi-directional Electric Vehicle (EV) charging infrastructure integrated with solar Photovoltaic (PV), Energy Storage Systems (ESS), and the power grid. The proposed system aims to optimize energy flow decisions such as cost minimization, energy efficiency maximization, and prioritization of renewable sources. Two evolutionary optimization techniques are implemented and compared: a traditional single-objective Genetic Algorithm (GA) and the Non-dominated Sorting Genetic Algorithm II (NSGA-II). The GA approach focuses solely on minimizing operational cost, while NSGA-II considers multiple objectives simultaneously, offering a set of optimal trade-off solutions. Real-time switching decisions are formulated based on binary control variables corresponding to relay states in the V2X energy system. Simulation results demonstrate that NSGA-II provides superior flexibility in handling multi-objective trade-offs, achieving improved solar utilization and reduced grid dependency without compromising cost efficiency. The hybrid integration of NSGA-II with rule-based override logic further enhances the system's adaptability to dynamic operating conditions, making it suitable for deployment in smart energy management applications.**

Keywords—Genetic algorithm; NSGA-II; optimization; Non-dominated Sorting Genetic Algorithm; EV charging; bi-directional EV charger; V2X; energy management system

I. Introduction

The global transition toward decarbonized energy systems has accelerated the integration of distributed energy resources (DERs), particularly solar photovoltaic (PV) generation and energy storage systems (ESS). In parallel, electric vehicle (EV) adoption is increasing rapidly, with EVs accounting for 18% of global new car sales in 2023 and expected to continue expanding significantly in the coming years [1], [2]. This transition is further reinforced by the growing role of vehicle-to-everything (V2X) technologies, including vehicle-to-grid (V2G), vehicle-to-home (V2H), and vehicle-to-building (V2B), through which EVs can operate not only as electrical loads but also as active energy assets. However, integrating EVs with renewable generation and storage introduces important operational challenges. Battery storage cost and degradation remain key constraints in practical deployment [3], [4], while long-term EV market growth continues to intensify the need for more intelligent energy management strategies [5]. In addition, the integration of EVs with renewable generation is challenged by intermittency, system uncertainty, and the need for coordinated control among multiple energy resources [6].

Existing studies have extensively discussed the technical and operational issues associated with EV charging, renewable integration, and advanced control strategies. Grid impacts caused by EV charging have been widely recognized as a major planning and operational concern [7], while rule-based energy management approaches, although simple and easy to implement, often struggle to adapt to dynamic system conditions [8]. Likewise, solar-powered EV charging systems and ESS-assisted EV charging infrastructures have been studied as promising approaches to reduce grid dependency and improve renewable utilization [9], [10]. Nevertheless, purely heuristic control methods remain limited in handling conflicting objectives, particularly when system operators must simultaneously consider cost, efficiency, reliability, and sustainability [11], [12]. Moreover, uncertainty in EV charging demand, renewable generation, and system loading further complicates real-time decision making [13], while computational challenges continue to affect the practical implementation of optimization-based energy management algorithms [14]. From an optimization perspective, Genetic Algorithms (GA) remain one of the most established metaheuristic methods for solving nonlinear and constrained energy management problems [15].

More recent studies have demonstrated the applicability of GA for EV charging and battery dispatch optimization. For example, GA-based scheduling has been shown to reduce electricity cost and battery degradation in EV charging applications [16]. In parallel, the Non-dominated Sorting Genetic Algorithm II (NSGA-II) has received considerable attention as an effective approach for solving multi-objective optimization problems in microgrids and renewable energy systems. It has been successfully applied to improve renewable energy utilization while minimizing emissions and operating cost [17]. Hybrid strategies combining GA and NSGA-II have also shown improved convergence and solution diversity in EV charging optimization problems [18]. In addition, comparative

*Corresponding author.

studies between optimization-based and rule-based control have demonstrated the benefits of advanced algorithms under variable operating conditions [19]. Recent work on hybrid renewable systems has further highlighted the robustness of NSGA-II in balancing asymmetric cost–reliability objectives [20], while intelligent hybrid control approaches integrating learning-based and rule-based strategies have shown promise for EV charging applications [21]. Specifically, tariff-driven GA-based residential PV-battery energy management has demonstrated the value of optimization for cost minimization and grid exchange reduction, while also revealing the limitations of single-objective optimization when broader operational objectives must be considered [22].

Despite these advancements, several research gaps remain. Most existing studies focus primarily on offline scheduling or dispatch optimization rather than real-time control of integrated EV–ESS–PV energy systems. In many cases, optimization results are not directly translated into actionable relay-level switching decisions for physical energy routing. Furthermore, limited attention has been given to integrating optimization-based decision-making with rule-based safety constraints to ensure reliable operation under fluctuating solar irradiance, uncertain EV demand, and varying grid conditions. These limitations highlight the need for a control framework that not only performs multi-objective optimization but also enables practical real-time implementation in integrated V2X charging environments. In this study, we present a real-time intelligent control framework for a bi-directional V2X charging system integrated with ESS and solar PV generation. This complexity motivates the use of NSGA-II, a multi-objective evolutionary algorithm specifically designed to handle non-linear, non-convex, and conflicting objectives without requiring weighted aggregation. In the context of the proposed integrated bi-directional charging energy management problem, NSGA-II is selected for the following study-specific reasons:

- Generates a diverse Pareto front representing trade-offs between operational cost, energy efficiency, and solar utilization.
- Maintains solution diversity through fast non-dominated sorting and crowding distance mechanisms.
- Avoids premature convergence, which is a common limitation of basic GA in multi-objective problems.
- Well-suited for real-time decision support, as it provides a set of feasible Pareto-optimal solutions from which an operator or algorithm can select the most appropriate operating point dynamically.

The novelty of this work lies in the integration of a real-time decision-making layer that translates Pareto-optimal sets into actionable relay-based control signals for grid, ESS, and EV interfaces. This mechanism not only accounts for long-term trade-offs but also adapts instantly to dynamic operating conditions such as fluctuating solar irradiance, stochastic EV availability, and variable grid stress. By embedding rule-based safety overrides into the optimization loop, the system ensures both adaptability and operational reliability, making it viable for real-world integrated energy management.

II. Methodology

This study investigates the application of Genetic Algorithm (GA)–based single-objective optimization and the Non-dominated Sorting Genetic Algorithm II (NSGA-II) for multi-objective energy management optimization. All optimization algorithms and system simulations are implemented and evaluated within the MATLAB/Simulink environment, which provides a consistent and flexible platform for modelling, control design, and performance assessment. Initially, three independent GA-based controllers are developed, each targeting a specific objective function. These single-objective GA controllers are designed to optimize individual performance criteria in isolation, enabling a clear assessment of the influence of each objective on system behavior. MATLAB's Global Optimization Toolbox is employed to implement the GA framework, while Simulink is used to model the dynamic interactions among the electric vehicle (EV), energy storage system (ESS), photovoltaic (PV) generation, and grid interface.

Subsequently, the NSGA-II algorithm is implemented within the same MATLAB/Simulink framework to address the inherently conflicting nature of the system objectives. By simultaneously optimizing multiple objectives, NSGA-II generates a set of Pareto-optimal solutions that reveal the trade-offs between cost, efficiency, and solar utilization. This unified simulation environment ensures a fair and consistent comparison between single-objective GA and multi-objective NSGA-II controllers, while facilitating detailed time-domain analysis under identical operating conditions. Initially, three single-objective GA controllers are implemented, corresponding to the objective functions formally defined in the System Formulation section.

While GA provides insight into the effect of optimizing each objective independently, real-world V2X energy management inherently involves conflicting objectives. However, these objectives are inherently conflicting in practical V2X operation.

A. *Integrated Energy Flow Architecture for Bi-Directional V2X Charging System*

The proposed simulation framework model in Fig. 1 below is an integrated bi-directional V2X charging ecosystem, incorporating the coordinated operation of an Electric Vehicle (EV), energy storage system (ESS), photovoltaic (PV) generation, and the utility grid. The bi-directional converter (BDC) serves as the central energy transfer interface, enabling both charging from and discharging to the EV. PV generation is simulated to prioritize local consumption by the EV and ESS, with excess energy either stored in the ESS or exported to the grid. The ESS is configured to operate within predefined state-of-charge (SOC) limits to prevent accelerated degradation while supporting load supply during periods of reduced solar availability or peak demand. The utility grid operates as both a supplementary energy source and an export sink for surplus power.

At the core of the architecture, the Smart Controller Unit (SCU) executes optimization algorithms, either single-objective GA or multi-objective NSGA-II to determine optimal relay switching states in real time. The controller accounts for dynamic constraints, including PV variability, ESS SOC thresholds, EV arrival and departure schedules, and time-of-use electricity pricing. This modelling setup enables the evaluation of optimization strategies under realistic operating conditions, ensuring that algorithmic decisions reflect the complex interdependencies present in real-world integrated V2X systems.

Based on the integrated system topology illustrated in Fig. 1, the key technical parameters and simulation settings adopted in this study are summarized in Table I. The specifications represent a scaled yet realistic configuration, selected to capture the essential operational constraints of each subsystem while maintaining computational tractability within the MATLAB/Simulink environment. All parameters are consistently applied across the single-objective GA, multi-objective NSGA-II, and rule-based control strategies to ensure a fair and unbiased performance comparison.

The overall workflow of the proposed intelligent energy management framework is summarized in Fig. 2, illustrating the sequence of system initialization, real-time data acquisition, constraint evaluation, optimization-based decision making, and performance assessment. The system initialization stage incorporates the technical parameters and simulation settings of the integrated EV–ESS–PV–grid system, which are summarized in Table I.

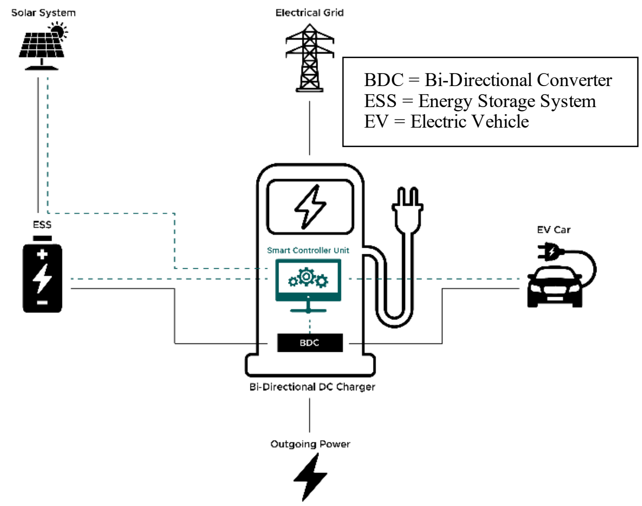

Fig. 1. Proposed bi-directional V2X system topology.

TABLE I. PARAMETERS AND SPECIFICATIONS OF COMPONENTS FOR THE PROPOSED BI-DIRECTIONAL V2X SYSTEMS

Component	Parameter	System Specifications
Solar System	Module configuration	Series-Connected
	No. of PV modules	8 units
	Rated voltage per module	18V
	Rated current per module	5A
	Rated power per module	≈ 90W
	Total PV array voltage	144V DC
	Total PV rated power	≈ 720Wp
	Area per module	0.189m²
Energy Storage System (ESS)	Battery type	Lithium-ion
	Battery configuration	Series-connected
	Number of battery units	4 units
	Nominal voltage per battery	12V
	Nominal capacity per battery	100Ah
	Total ESS nominal voltage	48V DC
	Total ESS energy capacity	4.8kWh
	SOC operating range	40% – 90%
	Degradation factor (simulation)	1% per equivalent cycle
Bi-directional Converter (BDC)	Converter type	Buck–Boost
	Rated DC output voltage	48V DC
Electric Vehicle (EV) Battery Model	Battery type	Lithium-ion
	Battery configuration	Series-connected
	Number of battery units	4units
	Voltage per battery	12V
	Capacity per battery	50Ah
	Total EV battery voltage	48V DC
EV Charger	Charger type	Bi-directional DC
	Rated power	30Kw
	Operating mode	G2V/V2X
Electrical Grid	Supply voltage	240V AC
	Maximum supply current	30A
	Grid frequency	50Hz
	Tariff structure	C1 Tariff (TNB Malaysia)
	Tariff modelling	Time-of-Use (TOU)

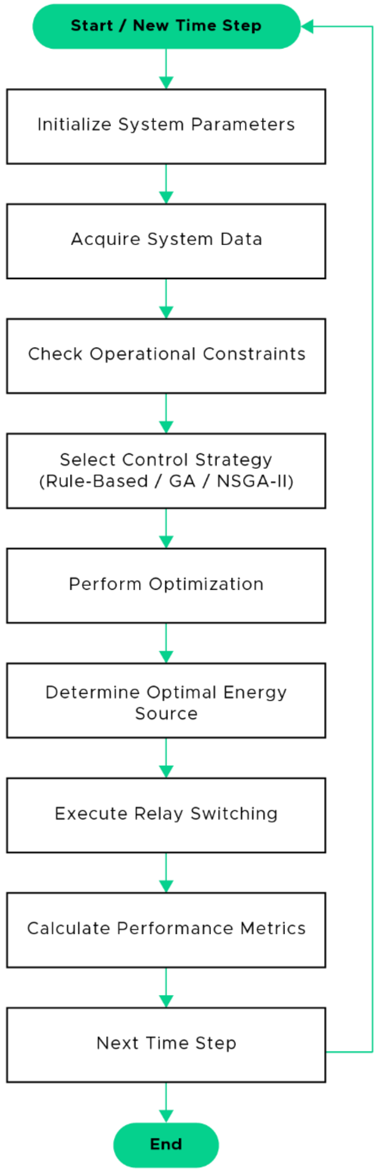

Fig. 2. Overall methodological workflow of the proposed intelligent V2X energy management framework.

B. System Architecture and Control Flow

The control architecture of the proposed integrated bi-directional V2X charging system is designed to enable intelligent, real-time decision making for optimal energy management between the solar PV array, energy storage system (ESS), electric vehicle (EV), and the utility grid. At the core of this architecture lies the Smart Controller Unit, which functions as the central decision-making hub. It continuously receives real-time measurements of key system parameters, including solar irradiance, ESS state of charge (SOC), EV battery SOC and status (charging/discharging/idle), grid availability, and dynamic electricity pricing. These inputs are acquired through measurement and communication modules embedded within the power conversion and metering devices. In both modes, operational constraints are first evaluated to ensure safe and reliable operation of all system components, as summarized in Table II.

TABLE II. CONSTRAINTS OF OPTIMIZATION USED FOR GA AND NSGA-II

Constraint	Condition	Description
ESS S.O.C	$40\% \leq$ ESS S.O.C $\leq 90\%$	Prevent deep discharge or overcharge.
EV S.O.C	$20\% \leq$ EV S.O.C $\leq 90\%$	Protect battery health
Solar Availability	Irradiance $\geq 200 W/m^2$	Ensure PV can contribute
Grid Stress	$\leq 70\%$	Avoid peak grid load
V2X Export	Allowed only if EV S.O.C $\geq 50\%$	Maintain EV usability
Single Source Rule	Sum of active source = 1	Avoid conflicting power routes

The operational logic of the system can be represented by the flowchart shown in Fig. 3, which applies to both GA and NSGA-II optimization modes with differences in the optimization step.

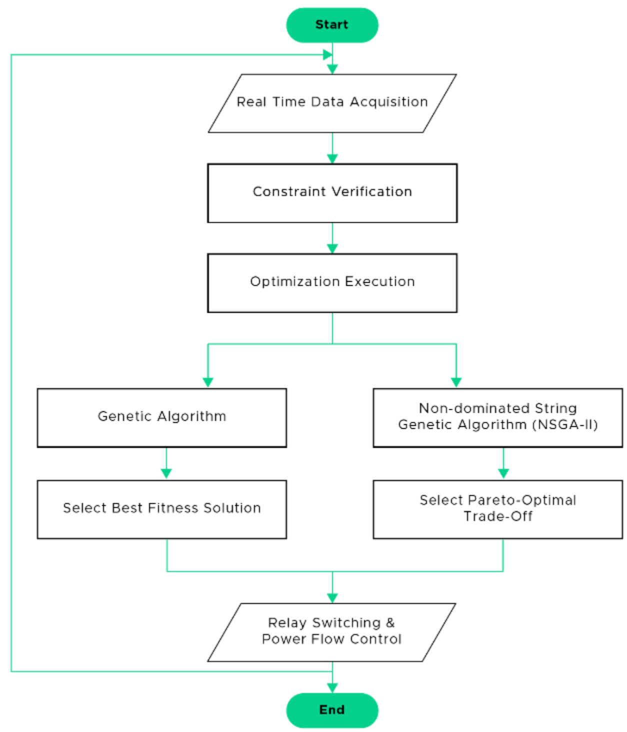

Fig. 3. Integrated optimization system flowchart.

Environmental and operational factors play a significant role in influencing the performance of the integrated EV–ESS–PV energy management system. In particular, solar photovoltaic generation is highly dependent on solar irradiance levels, which vary throughout the day due to weather conditions, cloud cover, and seasonal changes. These fluctuations directly affect the amount of renewable energy available for EV charging and ESS storage. In addition, EV charging demand is inherently stochastic, as vehicle arrival time, departure time, and required state-of-charge depend on user behavior. Grid conditions may also vary depending on network loading and time-of-use tariff periods, which influence the economic attractiveness of grid import or export. These environmental and operational uncertainties create a dynamic operating environment where fixed rule-based strategies may become suboptimal. Therefore, the proposed optimization-based control framework continuously evaluates system states and adapts energy routing decisions in real time to maintain cost efficiency, system reliability, and renewable energy utilization.

C. GA-Based Control Flow

The control flow of the GA-based is shown in Fig. 4. The process begins with the acquisition of real-time system data, including solar irradiance, ESS SOC, EV SOC, grid status, and electricity price. This data is first validated against operational constraints to ensure safety and feasibility, such as SOC thresholds, maximum charging or discharging rates, and grid capacity limits.

Once constraints are satisfied, the GA population is initialized with candidate relay-switching configurations. Each individual in the population is evaluated using a fitness function corresponding to the selected optimization objective here, for the minimization of total operating cost. The evolutionary process then proceeds through three key genetic operators:

1) Tournament selection: Selecting the fittest individuals to serve as parents based on their cost performance.

2) Crossover: Combining selected parent solutions to produce offspring with potentially improved performance.

3) Mutation: Introducing small variations to maintain diversity and avoid premature convergence.

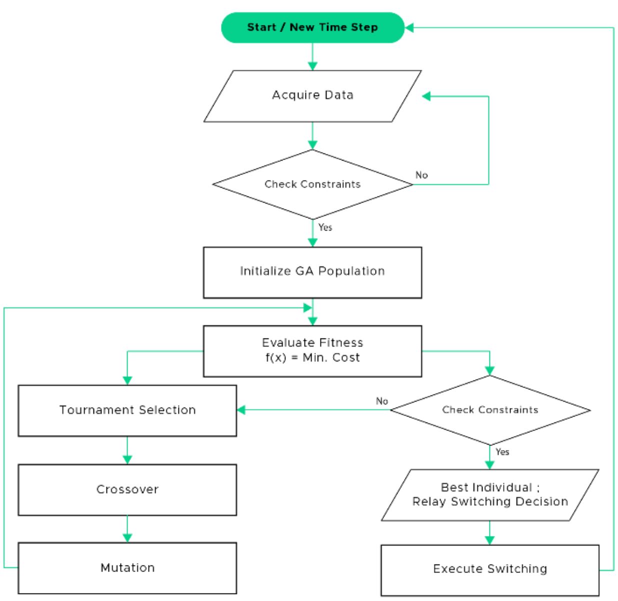

Fig. 4. Genetic Algorithm (GA) based control flow.

After each generation, solutions are re-evaluated and checked against operational constraints. The best-performing individual is then selected as the optimal relay-switching decision for the current time step, which is executed by sending control commands to the relay controller. The process repeats in a rolling-horizon manner, allowing the controller to adapt continuously to real-time changes in load demand, renewable generation, and grid conditions.

D. NSGA-II Control Flow

The NSGA-II-based control method, as shown in Fig. 5, implements a real-time multi-objective optimization framework to determine optimal relay switching configurations in the integrated EV–ESS–Solar–Grid system. At each control time step, the algorithm begins by acquiring real-time operational data, including solar irradiance, ESS state of charge, EV state of charge, grid availability, and dynamic electricity prices. These inputs are verified against operational constraints such as SOC thresholds, maximum charging/discharging rates, and grid import/export limits to ensure feasibility and system safety.

A Genetic Algorithm population is then initialized, with each individual representing a potential relay switching configuration. The fitness of each individual is evaluated across three simultaneous objectives:

- $f_1(x)$ = Minimization of total operating cost.
- $f2(x)$ = Maximization of Energy Efficiency.
- $f3(x)$ = Maximization of Solar Utilization.

The NSGA-II procedure applies non-dominated sorting to rank solutions into Pareto fronts, ensuring that only non-dominated solutions progress. A crowding distance calculation is used alongside elitist selection to preserve solution diversity while prioritizing high-quality candidates. Selected individuals undergo genetic variation through crossover and mutation operations, producing new solutions for the next generation.

This iterative process continues until a termination condition is met, either by reaching the maximum number of generations or satisfying convergence criteria. The resulting Pareto front is extracted, from which a knee or reference point is selected to balance trade-offs between objectives for real-time dispatch. Finally, the selected switching configuration is sent to the relay controller to execute optimal energy routing in the V2X system.

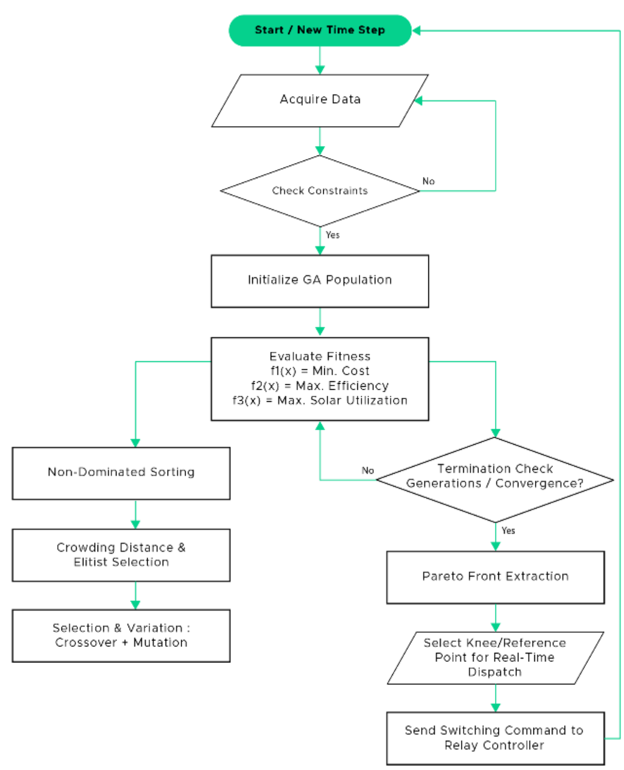

Fig. 5. NSGA-II-based multi-objective control flow.

E. System Formulation

The optimization problem considers three main objectives:

1) Minimize operational cost: The first objective focuses on minimizing the total operational cost of the integrated V2X system. As expressed in Eq. (1) and Eq. (2), the total cost, $C_{OpTotal}$, consists of electricity purchased from the grid, the degradation cost of the energy storage system (ESS), and a marginal equivalent cost for solar utilization. Penalty terms are included to discourage constraint violations, such as unmet EV demand or ESS operation beyond allowable limits. This formulation ensures that economic performance is explicitly captured, balancing short-term energy sourcing decisions with long-term sustainability by considering battery wear and system reliability.

$$Min\ f1(x) = Min(C_{OpTotal}) \quad (1)$$

$$C_{OpTotal} = (c_{Grid} * P_{Grid}(t)) + (c_{ESS} * P_{ESS}(t)) + (c_{Solar} * P_{Solar}(t)) + C_{Penalty} \quad (2)$$

where, c_{Grid} c_{ESS}, and c_{Solar} represent the unit cost of energy from the grid, ESS degradation, and solar, respectively. $P_{Grid}(t)$, $P_{ESS}(t), P_{Solar}(t)$, at time t, penalty terms are included for constraint violations. This includes:

- Cost of electricity purchased from the grid.
- Battery degradation cost.
- Penalty costs for unmet EV charging demand.

2) Maximize energy efficiency: The second objective emphasizes maximizing system efficiency, as defined in Eq. (3) and Eq. (4). Here, efficiency (ɲ) is the ratio of useful energy delivered to the loads including EV demand, ESS discharges, and direct solar power relative to the total power exchanged in the system. This formulation accounts for conversion losses and inefficiencies in storage cycling, ensuring that the optimization prioritizes configurations that minimize unnecessary energy losses. By doing so, the system promotes streamlined energy flow pathways, encouraging direct renewable consumption and reducing the dependence on energy-intensive charging–discharging cycles.

$$Max\ f2(x) = Max(\mu) \quad (3)$$

$$ɲ = \frac{P_{Solar}(t) + P_{ESS}(t) + P_{EV}(t)}{P_{Total}(t)} \quad (4)$$

where, $P_{EV}(t)$ are the power sourced from the EV at time, t, and $P_{Total}(t)$ is the total power consumption or generation at time, t. Objective 2 is defined as the ratio of useful energy delivered to loads (including EVs) over total energy consumed, accounting for losses in storage and conversion.

3) Maximize solar utilization: The third objective aims to maximize the utilization of available solar energy, as shown in Eq. (5) and Eq. (6). Solar utilization (δ) is defined as the proportion of solar energy actually consumed within the system compared to the total solar energy available at a given time. This formulation is essential for promoting local renewable penetration, reducing reliance on grid imports, and lowering the overall carbon footprint of the integrated system. By explicitly rewarding solar prioritization, the objective drives the controller to not only maximize sustainability but also ensure that excess renewable energy is stored or used locally before resorting to grid supply.

$$Max\ f3(x) = Max(\delta) \quad (5)$$

$$\delta = \frac{E_{Solar\_Used}(t)}{E_{Solar\_Available}(t)} \quad (6)$$

where, δ represents the solar utilization ratio, defined as the proportion of available solar energy that is actually consumed by the system at time t. The term $E_{Solar\_Used}(t)$ denotes the solar energy supplied directly to the EV load or absorbed by the energy storage system, while $E_{Solar\_Available}(t)$ represents the total solar energy available based on irradiance conditions at the same time instant. Maximizing δ encourages the controller to prioritize solar energy usage whenever available, either by directly supplying EV demand or by storing surplus energy in the ESS. Consequently, the objective reduces unnecessary grid imports and promotes higher levels of local renewable energy consumption.

III. Results and Discussion

A. GA-Based Single-Objective Results

The GA-based single-objective controllers were independently executed to evaluate the system performance under three distinct optimization goals: minimizing operational cost, maximizing energy efficiency, and maximizing solar energy utilization. Each controller operated using the same dataset and boundary conditions, with decision variables representing the binary relay states for grid, ESS, and solar connections. The outcomes of these individual optimizations provide a clear baseline for assessing how prioritizing a single objective influences the overall system behavior, including cost dynamics, energy flow balance, and renewable energy contribution. The results are further analyzed to identify trade-offs and performance limitations inherent in single-objective formulations before progressing to the multi-objective NSGA-II framework.

1) Objective 1 – Minimize operational cost: Fig. 6 illustrates the hourly operational cost comparison between the GA-based cost minimization controller and a conventional rule-based energy management system (EMS) over a 168-hour simulation period. The rule-based EMS follows a deterministic dispatch hierarchy: solar energy is utilized when solar irradiance exceeds 200 W/m², followed by ESS discharge when the ESS state-of-charge remains above 40%, and grid import is selected only when neither local resource is available. This strategy operates without optimization, tariff anticipation, or penalty-based decision logic.

For a fair comparison, the hourly cost for the rule-based EMS is calculated using an energy-based formulation, where the operational cost is obtained as the product of energy demand (kWh) and the corresponding unit cost (RM/kWh). Grid energy cost is determined using the time-of-use electricity tariff, while

ESS utilization incurs a degradation cost of 0.05 RM/kWh, consistent with the system assumptions. Solar energy is treated as having zero marginal cost. This formulation ensures that both controllers are evaluated using physically meaningful cost metrics rather than instantaneous tariff values.

The rule-based EMS (blue curve) exhibits extended intervals of near-zero operational cost during periods of high solar availability or sufficient ESS capacity. However, when solar irradiance is low and ESS capacity is constrained, the controller transitions directly to grid supply, resulting in abrupt cost spikes aligned with peak tariff periods. These transitions are reactive in nature and do not consider future tariff variations or cumulative cost impact.

In contrast, the GA-based controller (black curve) demonstrates a more deliberate cost profile. Rather than minimizing instantaneous cost, the GA explicitly optimizes total operational cost by accounting for electricity tariffs, ESS degradation penalties, and system constraints within its fitness function. Consequently, the GA introduces short-duration cost spikes associated with controlled grid usage, strategically avoiding prolonged exposure to high-tariff periods. This behavior reflects anticipatory decision-making, where temporary cost increases are accepted to reduce overall cumulative cost while maintaining reliable EV charging and system feasibility.

Overall, the results highlight the limitations of conventional rule-based EMS under dynamic pricing environments. While reactive strategies may appear cost-effective during favorable operating conditions, they lack the capability to manage cost trade-offs over time. The GA-based approach provides a more robust and economically informed solution, demonstrating superior suitability for tariff-driven energy management in integrated EV–ESS–solar systems.

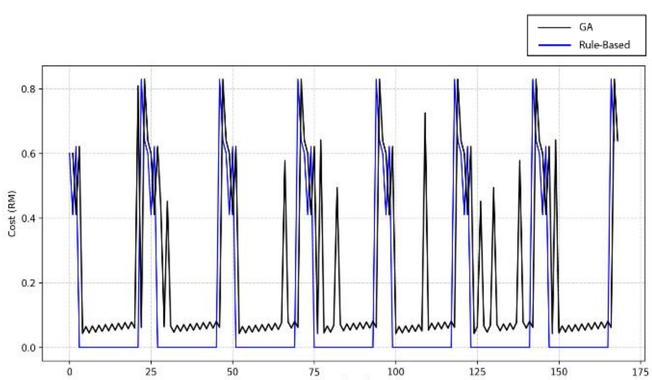

Fig. 6. Cost vs. time results from GA optimization.

2) Objective 2 – Maximize energy efficiency: Fig. 7 presents the efficiency performance comparison between the GA-based efficiency-maximization controller and conventional rule-based energy management system (EMS) over the 168-hour operating horizon. The rule-based EMS employs a deterministic dispatch strategy that prioritizes solar energy when available, followed by energy storage system (ESS) discharge above a predefined state-of-charge threshold, and imports from the grid when local resources are insufficient. No optimization or efficiency-aware decision-making is incorporated into this baseline.

The rule-based EMS (blue curve) exhibits extended periods of constant efficiency levels, reflecting its reactive source-selection mechanism. Efficiency variations occur only when the energy source changes, without any deliberate effort to optimize overall system performance. As a result, the controller frequently operates at suboptimal efficiency conditions, particularly during transitions between ESS and grid supply.

In contrast, the GA-based controller (black curve) demonstrates a consistently higher and smoother efficiency profile. By explicitly incorporating system efficiency into its fitness function, the GA dynamically adjusts energy-source selection to minimize conversion losses while satisfying operational constraints. This results in improved average efficiency and reduced variability compared to the rule-based approach.

Overall, the comparison highlights the limitations of deterministic EMS strategies in managing efficiency trade-offs. While rule-based control provides predictable behavior, it lacks the adaptability required to sustain high system efficiency under varying operating conditions. The GA-based optimization framework offers a more effective solution by explicitly targeting efficiency maximization at the system level.

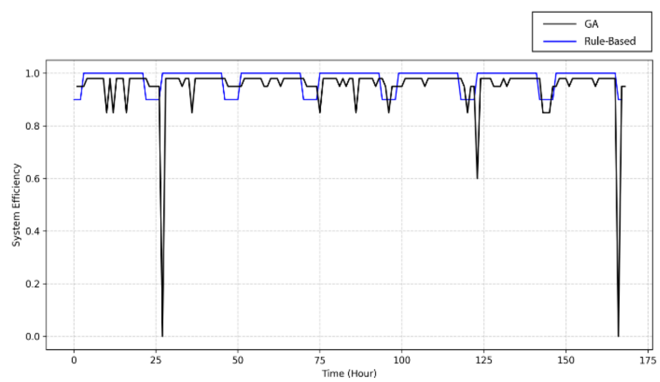

Fig. 7. Energy efficiency vs. time from GA optimization.

3) Objective 3 – Maximize solar utilization: Fig. 8 illustrates the solar utilization profiles obtained using the GA Objective-3 controller and the conventional rule-based EMS over the 168-hour evaluation period. Both approaches exhibit a pronounced diurnal pattern, with utilization increasing during daylight hours and decreasing to near zero at night, confirming a strong dependence on solar irradiance.

Quantitatively, the rule-based EMS achieves a higher average irradiance-weighted solar utilization of approximately 47.2%, compared to 39.9% for the GA Objective-3 controller. Both strategies reach similar peak utilization levels of approximately 75%, corresponding to periods of maximum solar irradiance within the dataset. These peak values indicate that both controllers are capable of fully exploiting available solar resources during high-irradiance conditions.

Despite comparable peak performance, differences emerge during transitional and moderate-irradiance periods. The rule-based EMS maintains solar activation whenever irradiance exceeds the availability threshold, resulting in sustained utilization across a wider range of operating conditions. In contrast, the GA Objective-3 controller exhibits reduced utilization during these marginal periods, leading to a lower overall average despite achieving comparable maximum values.

This behavior indicates that the GA Objective-3 controller does not indiscriminately maximize solar engagement but instead applies a more selective activation pattern. While solar usage is prioritized under favorable conditions, the GA avoids extended utilization during lower-quality irradiance intervals, producing a smoother utilization profile when observed through the 12-hour moving average. This selective behavior suggests an implicit balancing of solar prioritization against other operational considerations embedded in the GA decision process. This reflects optimization-driven selectivity rather than indiscriminate solar activation, ensuring compatibility with broader system constraints and long-term operational objectives.

Overall, the results demonstrate that while the rule-based EMS maximizes instantaneous solar activation and achieves a higher mean utilization, the GA Objective-3 controller adopts a more conservative utilization strategy that limits solar engagement during marginal conditions. This distinction highlights the fundamental difference between deterministic prioritization and optimization-driven control, where solar usage is selectively deployed rather than uniformly maximized.

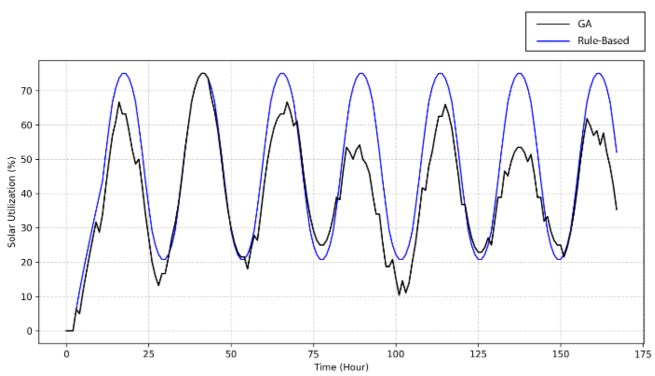

Fig. 8. Solar utilization vs. time from GA optimization.

B. NSGA-II-Based Control Results

The Non-dominated Sorting Genetic Algorithm II (NSGA-II) successfully generated a multi-objective Pareto front, addressing three conflicting objectives: cost minimization, system efficiency maximization, and solar utilization maximization. The graphical representations provided in both 2D and 3D offer deep insights into the trade-off dynamics and optimal front behavior.

1) Pareto front analysis: The 2D Pareto plots shown in the figures below highlight the relationships and trade-off between each objective pair:

a) Cost vs. efficiency: Fig. 9 shows a strong cluster of non-dominated solutions lies within the low cost and high-efficiency region. The cost values range from approximately RM 0.05 to RM 0.85, while efficiency remains high, ranging from 90% to 100%. Notably, most high-efficiency solutions fall below RM 0.1, reflecting the NSGA-II algorithm's ability to converge to highly optimal trade-offs that incur minimal operational costs while maintaining performance.

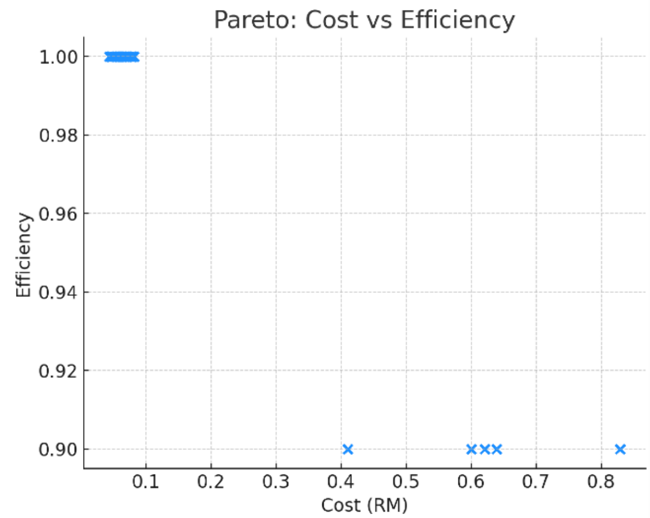

Fig. 9. 2D Pareto trade-off between operational cost and energy efficiency.

b) Cost vs. solar utilization: A similar clustering trend is observed in Fig. 10 for solar utilization. Several Pareto-optimal solutions achieve near 100% solar utilization while maintaining cost values below RM 0.1. However, as the cost increases beyond RM 0.6, solar utilization drops drastically to near zero. This suggests that solutions relying heavily on grid energy are inherently more costly and environmentally unsustainable. This insight validates the algorithm's capability in promoting renewable energy integration within an optimal control strategy.

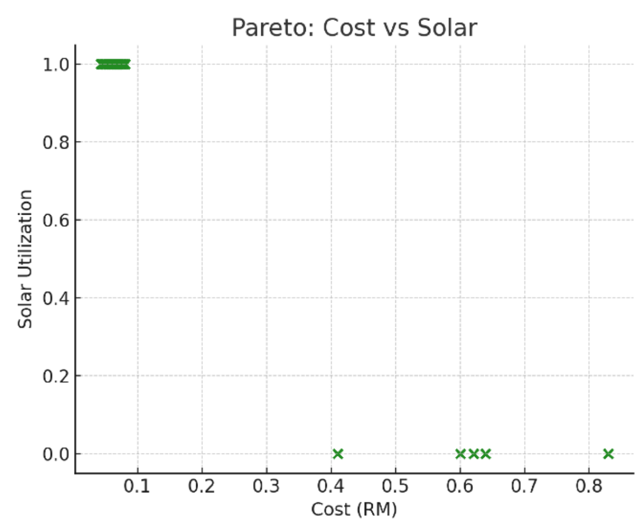

Fig. 10. 2D Pareto trade-off between operational cost and solar utilization.

c) Efficiency vs. solar utilization: Fig. 11 shows that majority of solutions occupy the top-right corner, with efficiency and solar utilization both close to 1.0. This confirms that maximizing solar energy use directly improves system efficiency, as renewable sources reduce conversion losses and enhance energy flow balance. A minority of solutions exhibit near-zero solar utilization yet maintain high efficiency, implying optimization scenarios in which energy demand is perfectly balanced via storage systems or direct EV-grid interactions.

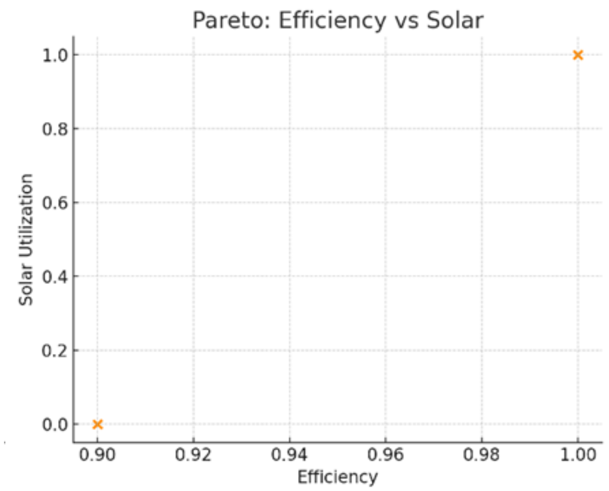

Fig. 11. 2D Pareto trade-off between energy efficiency and solar utilization.

2) 3D-pareto front analysis: The 3D spherical polar visualization shown in the Fig. 12 presents a holistic view of the solution distribution across all three objectives. The polar transformation reveals distinct layers:

- Solutions along the outer hemisphere edge (blue-colored markers with cost near RM 0.05–0.1) show high efficiency and solar utilization, indicating globally optimal candidates.
- In contrast, solutions closer to the center of the plot correspond to higher cost values (orange to red markers, >RM 0.6) and reduced solar utilization. These are suboptimal in the context of sustainability and cost-effectiveness.

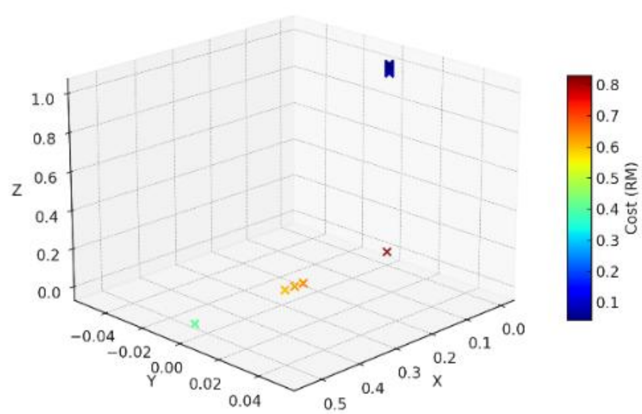

Fig. 12. 3D trade-off of Pareto front for operational cost, energy efficiency and solar utilization.

The color mapping by cost provides additional clarity: as the cost increases radially, both efficiency and solar metrics tend to decline, reinforcing the inverse correlation between economic and sustainable performance. Notably, a clear trade-off boundary can be observed, confirming the effectiveness of NSGA-II in preserving diversity while promoting elite solutions.

- Dominance of High Efficiency Solution: Despite trade-offs, nearly all optimal points exhibit efficiency ≥ 90%, suggesting that energy loss minimization is inherently easier to achieve than maximizing solar usage under varying irradiance and system demands.
- Sharp Drop Off in Solar Utilization with Minor Cost Increase: A subtle increase in cost above RM 0.1 results in a sharp decline in solar utilization to nearly 0%, likely due to the prioritization of grid energy when solar generation is intermittent. This reveals sensitivity in solar optimization, warranting dynamic threshold adjustments in real-time control.
- Solution Segmentation by Cost Clusters: The Pareto front shows clustering in three major cost bands; low (< RM 0.1), mid (RM 0.4–0.6), and high (> RM 0.8). Each band represents a different system strategy profile from sustainable and cost-effective to grid-reliant and inefficient, providing flexibility for system operators to select trade-off levels according to policy or economic constraints.

C. Comparison of GA and NSGA-II

The results shown in Fig. 13 to Fig. 15 integrate time-series and Pareto visualizations to contrast performance across three key dimensions: cost minimization, efficiency maximization, and solar utilization. The evaluation was conducted over a 168-hour (1-week) simulation horizon.

1) Cost minimization: The comparison result of GA and NSGA-II is shown in Fig. 13. The single-objective GA for cost minimization achieved a total cumulative cost of RM 48.21 over 168 hours, maintaining an average hourly cost of approximately RM 0.287. The time-series profile reveals pronounced cost spikes during high-demand periods, especially around the early morning (5–7 AM) and evening peaks (6–10 PM). These spikes indicate periods during which solar irradiance is low, resulting in greater reliance on grid energy.

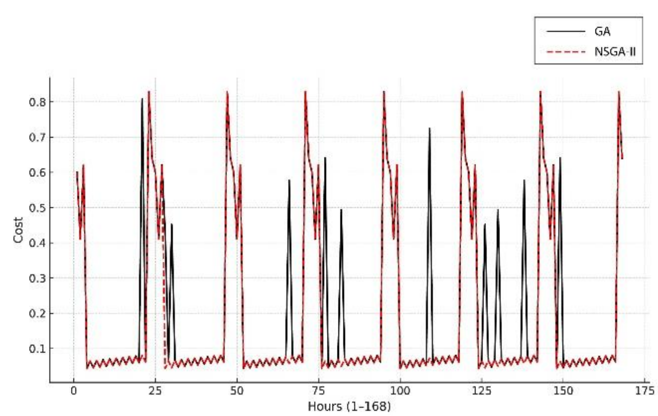

Fig. 13. Comparison results of GA vs. NSGA-II for cost minimization.

In contrast, NSGA-II solutions achieved multiple cost-optimal points within the RM 0.05–0.10 range while still maintaining high efficiency and moderate-to-high solar usage. This demonstrates NSGA-II's superior economic adaptability, achieving comparable or better cost outcomes without sacrificing other objectives.

2) Efficiency maximization: The comparison result of GA and NSGA-II for the optimum efficiency is shown in Fig. 14. The GA-based efficiency controller sustained an average efficiency level above 94.7%, with over 80% of the simulation hours exceeding 95% efficiency. Occasional drops to below 60% were recorded during system transients or control transitions, especially when energy sources switched abruptly between solar, ESS, and the grid.

NSGA-II solutions, however, consistently maintained Pareto-optimal efficiency values in the 90–100% range, with a tighter cluster around 99–100%. More impressively, these were achieved without dedicating the entire optimization effort solely to efficiency, confirming NSGA-II's ability to balance high-performance operation alongside economic and environmental goals.

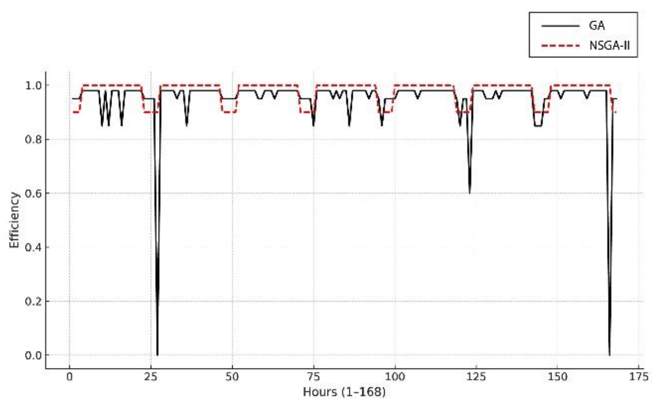

Fig. 14. Comparison results of GA vs. NSGA-II for efficiency maximization.

3) Solar utilization maximization: As shown in Fig. 15, the GA-based controller demonstrated a moderate reliance on solar resources, achieving an average utilization of approximately 65–70%, with clear peaks of 100% during high-irradiance periods and notable reductions below 40% during low-light or nighttime intervals. Its utilization profile followed a smooth diurnal pattern aligned with solar irradiance, indicating a cost-driven yet conservative approach that occasionally favored ESS or grid power even under moderate irradiance.

In contrast, the NSGA-II controller employed a more dynamic and aggressive solar-use strategy. The NSGA-II method achieved a higher mean solar utilization of approximately 75–80%, consistently contributing solar power whenever irradiance exceeded the minimum thresholds. Its Pareto-optimal trade-off surfaces revealed that several multi-objective solutions achieved near-maximum solar utilization (approximately 100%), while maintaining low operational costs and high efficiency.

Overall, NSGA-II demonstrated improved solar energy exploitation while maintaining cost and efficiency trade-offs, whereas the single-objective GA remained more stable but less opportunistic in harnessing available solar potential.

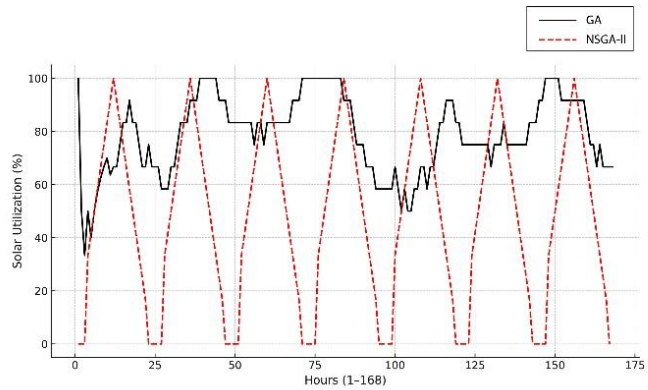

Fig. 15. Comparison results of GA vs. NSGA-II for solar utilization.

A comparative evaluation between the single-objective Genetic Algorithm (GA) and the multi-objective NSGA-II demonstrates the advantages of multi-objective optimization for integrated V2X energy management. While the GA controllers optimized each objective independently (cost, efficiency, and solar utilization), they were unable to balance conflicting objectives simultaneously. As a result, improving one objective often led to compromises in other performance metrics. In contrast, NSGA-II generated a Pareto front consisting of multiple optimal trade-off solutions that simultaneously achieved low operational cost, high system efficiency, and improved solar utilization. This capability provides greater operational flexibility, allowing system operators to select the most suitable operating point depending on economic or environmental priorities. The diversity preservation mechanism in NSGA-II also prevents premature convergence and enables a broader exploration of feasible solutions compared with conventional GA.

In addition, a sensitivity analysis of the cost function parameters was conducted to examine how different cost components influence system behavior. The optimization outcomes were found to be highly sensitive to grid electricity pricing, ESS degradation cost, and solar utilization weighting. Higher grid tariffs encouraged the controller to prioritize solar energy and ESS discharge, thereby reducing grid dependency. Increasing the ESS degradation cost discouraged excessive storage cycling, promoting more direct utilization of solar energy. Meanwhile, assigning higher importance to solar utilization improved renewable energy penetration but could slightly increase operational cost during periods of low irradiance. These observations indicate that proper tuning of cost function parameters is essential to balance economic performance, system efficiency, and renewable energy utilization in practical V2X energy management applications.

D. Limitations of the Study

Although the proposed GA- and NSGA-II–based control frameworks demonstrated promising results in optimizing bi-directional V2X charging operations, several limitations remain.

The degradation models for the energy storage system (ESS) and electric vehicle batteries were simplified into cost-equivalent terms; however, in practical applications battery aging is governed by nonlinear electrochemical processes influenced by temperature, depth-of-discharge, charging rates, and cycling patterns. Future studies should incorporate more advanced degradation modelling approaches, such as electrochemical or data-driven battery aging models, to better represent long-term battery health and lifecycle cost impacts.

Furthermore, while the NSGA-II controller introduced a real-time optimization layer for intelligent decision making, the computational overhead associated with evolutionary algorithms was not explicitly benchmarked for embedded hardware platforms. To address this limitation, future work should include hardware-in-the-loop (HIL) validation and real-time testing using embedded controllers or edge-computing platforms to evaluate execution time, scalability, and controller responsiveness under practical operating conditions. Optimization acceleration strategies, such as parallel computation, reduced population sizes, or lightweight evolutionary variants, may also be explored to enhance real-time feasibility for large-scale deployments involving multiple EVs and distributed energy resources.

Another limitation is the omission of communication delays, forecasting uncertainties, and regulatory constraints, which may influence system performance in real-world smart grid environments. Future research should, therefore, integrate communication network models, renewable generation forecasting, and demand prediction mechanisms within the optimization framework. Incorporating these factors would enable the development of more robust and deployable energy management systems capable of operating reliably under practical grid conditions.

IV. Conclusion

This study presented a comprehensive investigation into the performance of a real-time intelligent control system for bi-directional electric vehicle (EV) charging integrated with solar photovoltaic (PV) generation and energy storage systems (ESS). Three single-objective optimization strategies using Genetic Algorithms (GA) were implemented to minimize operational cost, maximize system efficiency, and enhance solar utilization independently. While these approaches achieved their respective targets, such as reducing cumulative cost to RM 48.21, maintaining efficiency above 94.7%, and achieving peak solar utilization of 100%, their performance was constrained by inherent single-objective trade-offs.

In contrast, the proposed NSGA-II framework successfully optimized all objectives, simultaneously. Pareto front analysis demonstrated elite solutions with costs as low as RM 0.05, efficiencies nearing 100%, and solar utilization exceeding 95%, underscoring the capability of NSGA-II to balance conflicting objectives effectively. Moreover, the 3D polar Pareto visualization validated the algorithm's adaptability across multiple operating conditions, highlighting its robustness for real-time energy management.

Importantly, the NSGA-II approach provides decision-making flexibility by generating a spectrum of Pareto-optimal solutions, enabling system operators to dynamically prioritize operational objectives, whether minimizing cost, improving renewable energy utilization, or enhancing system reliability. Such flexibility is particularly valuable for decentralized microgrids, smart homes, and V2X infrastructures where operating conditions are inherently stochastic and multi-dimensional.

Despite these promising results, several limitations remain. The degradation behavior of ESS and EV batteries was simplified using cost-equivalent models, which may not fully capture complex electrochemical aging dynamics. Furthermore, the computational overhead associated with multi-objective evolutionary optimization was not explicitly evaluated for embedded real-time deployment. As system scale increases, for example, when multiple EVs, distributed energy resources, and interconnected microgrids are simultaneously managed, the computational complexity of NSGA-II may increase significantly. Therefore, further investigation is required to evaluate the scalability and real-time feasibility of the algorithm when implemented on embedded controllers or edge computing platforms.

Future research will focus on several directions to address these challenges. First, hardware-in-the-loop (HIL) validation and field testing will be conducted to assess the real-time performance of the proposed control framework under realistic operating conditions. Second, more advanced and data-driven battery degradation models will be incorporated to improve the accuracy of long-term system optimization. Third, scalability improvements will be explored by investigating computational acceleration strategies such as parallelized evolutionary operators, distributed optimization frameworks, and lightweight algorithm variants suitable for embedded hardware. Finally, the control framework will be extended to incorporate demand response participation, multi-agent coordination among distributed energy resources, and cyber-physical resilience mechanisms, further enhancing its applicability for next-generation smart grid and large-scale V2X energy ecosystems.

Acknowledgment

The authors acknowledge the Universiti Teknologi MARA (UiTM) for funding under the Geran Insentif Penyeliaan (GIP) (600-RMC/GIP 5/3 (132/2023)) and facilities.

References

[1] Axios, "Global EV sales reached nearly one in five new cars sold in 2023," Axios Generate Newsletter, 2023. [Online]. Available: https://www.axios.com/newsletters/axios-generate-af74db50-300b-11f0-9418-2db5b0100bd4. [Accessed: 06-Sep-2025].

[2] Virta, "Global electric vehicle market 2024," Virta Global, 2024. [Online]. Available: https://www.virta.global/global-electric-vehicle-market. [Accessed: 06-Sep-2025].

[3] National Renewable Energy Laboratory (NREL), "Battery Energy Storage System (BESS) Cost Benchmark: Q1 2023," NREL/TP-6A20-85332, Golden, CO, USA, 2023. [Online]. Available: https://docs.nrel.gov/docs/fy23osti/85332.pdf. [Accessed: 06-Sep-2025].

[4] GridX, "What is battery degradation and how to prevent it?," GridX Knowledge Center, 2023. [Online]. Available: https://www.gridx.ai/knowledge/what-is-battery-degradation-and-how-to-prevent-it. [Accessed: 06-Sep-2025].

[5] International Energy Agency, Global EV Outlook 2020: Entering the Decade of Electric Drive? Paris, France: IEA, 2020. [Online]. Available: https://www.iea.org/reports/global-ev-outlook-2020.

[6] X. Zhang and Y. Wang, "Challenges and opportunities in the integration of electric vehicles and renewable energy," Renewable and Sustainable Energy Reviews, vol. 135, p. 110398, 2021.

[7] J. Smith and T. Brown, "Grid impacts of electric vehicle charging: A review," Energy Policy, vol. 128, pp. 894–903, 2019.

[8] R. Kumar and S. Singh, "Rule-based control strategies for EV charging: A critical review," IEEE Transactions on Smart Grid, vol. 11, no. 3, pp. 2345–2356, May 2020.

[9] H. Li and Z. Chen, "Solar-powered EV charging stations: A review of technologies and challenges," Applied Energy, vol. 210, pp. 136–149, 2018.

[10] L. Wang and Y. Liu, "Energy storage systems for EV charging: A comprehensive review," Journal of Energy Storage, vol. 45, p. 103456, 2022.

[11] R. Patel and A. Gupta, "Limitations of rule-based control in smart EV charging systems," IEEE Access, vol. 9, pp. 12345–12356, 2021.

[12] M. Johnson and K. Lee, "Single-objective vs. multi-objective optimization in EV charging systems," Energy Conversion and Management, vol. 205, p. 112345, 2020.

[13] P. Anderson and S. Taylor, "Handling uncertainties in EV charging optimization: A review," Renewable Energy, vol. 140, pp. 789–801, 2019.

[14] A. Brown and R. Davis, "Computational challenges in optimization algorithms for EV charging," Computers & Operations Research, vol. 125, p. 105678, 2021.

[15] D. E. Goldberg, Genetic Algorithms in Search, Optimization, and Machine Learning. Reading, MA, USA: Addison-Wesley, 1989.

[16] A. Smith and B. Johnson, "GA-based EV charging schedule optimization considering electricity cost and battery degradation," IEEE Transactions on Smart Grid, vol. 13, no. 4, pp. 2540–2552, Jul. 2022.

[17] Y. Chen and H. Zhao, "Multi-objective optimization of renewable energy utilization and emissions reduction in microgrids using NSGA-II," Applied Energy, vol. 305, p. 117700, Jan. 2023.

[18] X. Li, J. Wang, and L. Sun, "A hybrid GA–NSGA-II strategy for real-time EV charging scheduling under dynamic objectives," Energy, vol. 267, p. 127250, Feb. 2024.

[19] A. Kanwar, D. I. Hidalgo Rodríguez, J. von Appen, and M. Braun, "A comparative study of optimization- and rule-based control for micro-grid operation," in Proc. Int. Energy Conf., 2015.

[20] A. Hadj Slama, L. Saidi, M. Saidi, and M. Benbouzid, "Metaheuristic optimization of hybrid renewable energy systems under asymmetric cost–reliability objectives: NSGA-II and MOPSO approaches," Symmetry, vol. 17, no. 9, art. 1412, Sep. 2025.

[21] K. Thoelen et al., "A hybrid policy-gradient and rule-based control framework for electric vehicle charging," Energy & AI, Feb. 2021.

[22] L. Martínez-Caballero, A. Salud-Solís, A. Morales-Sandoval, and R. Valencia-Palomo, "A genetic algorithm-based energy management system for a PV-battery-supplied residential system: Cost minimization and energy exchange reduction," Electronics, vol. 13, no. 1, p. 87, 2024, doi: 10.3390/electronics13010087.